INTERNATIONAL JOURNAL FOR NUMERICAL METHODS IN FLUIDS
Int. J. Numer. Meth. Fluids 2008; **57**:677–692
Published online 11 September 2007 in Wiley InterScience (www.interscience.wiley.com). DOI: 10.1002/fld.1588

Molecular dynamics study of the interaction of a shock wave with a biological membrane

Javier Lechuga[1], Dimitris Drikakis[1,*,†] and Sandip Pal[2]

[1]*Cranfield University, Fluid Mechanics and Computational Science Group (FMaCS), Aerospace Sciences, Bedfordshire MK43 0AL, U.K.*
[2]*Mid Essex NHS Trust, Broomfield Hospital, Essex, U.K.*

SUMMARY

This paper presents a computational study of the interaction of a shock wave with a biological membrane. The membrane model comprises 21 555 atoms which build 66 dalmitoyloleoylphosphatidylcholine (POPC) lipids forming the bilayer, and 4237 water molecules, with the distance between the layers being set to fit around the actual membrane thickness (54 Å), and the lattice period being set to fit the actual surface density of lipid molecules. We have employed a molecular dynamics method for solving the Newton equations of motion numerically thereby providing a strategy to understand the basic physics of the biological structure at atomistic level. A shock wave has been modelled as an impulse of 40 Pa s, and simulations for the interaction of the shock wave with the membrane have been performed for 200 ps to investigate the different effects of the shock wave on different membrane properties including thickness, area, volume, order parameter and lateral diffusion. Copyright © 2007 John Wiley & Sons, Ltd.

Received 27 October 2006; Revised 15 June 2007; Accepted 19 June 2007

KEY WORDS: shock wave; biological membrane; molecular dynamics; diffusion; mass transport; nanoscience

1. INTRODUCTION

According to the currently accepted theory, known as the fluid mosaic model (Figure 1) [1], the plasma membrane consists of a double layer (bilayer) of lipids, which are oily substances found in all cells. Most of the lipids in the bilayer can be more precisely described as phospholipids, i.e. lipids that feature a phosphate group at one end of each molecule. The phospholipids, the most abundant molecules in the membrane, have a hydrophilic head and a hydrophobic tail. The

*Correspondence to: Dimitris Drikakis, Cranfield University, Fluid Mechanics and Computational Science Group (FMaCS), Aerospace Sciences, Bedfordshire MK43 0AL, U.K.
†E-mail: d.drikakis@cranfield.ac.uk

Contract/grant sponsor: HEAL Cancer Charity

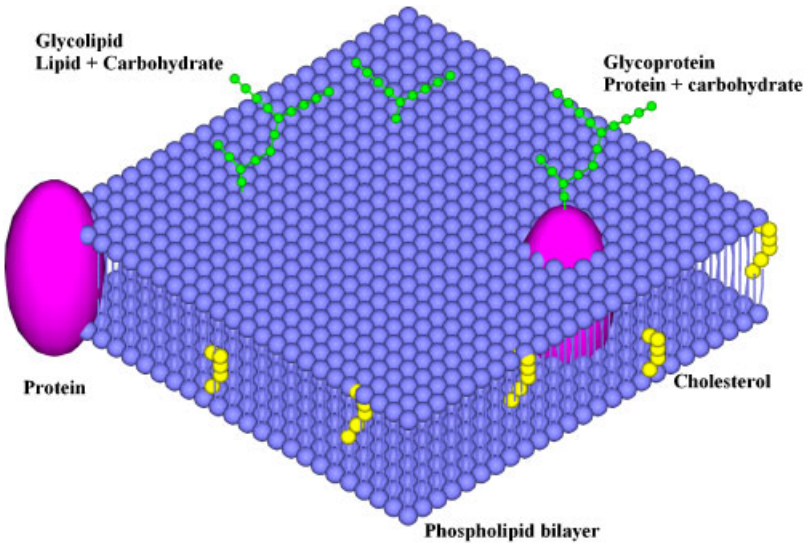

Figure 1. Fluid mosaic model [1].

tails of each lipid layer are in contact inside the cell membrane as the polar heads contact the extracellular fluid and the intracellular cytoplasm. This structure is fluid, so molecules can move around within the bilayer. In fact, this is a complex biological system which serves as a barrier between the extracellular fluid and the intracellular cytoplasm. However, its functions go beyond that, as it controls the uptake of molecular substances into the cell, and the interactions among the membrane molecules are crucial in the cellular metabolism.

A biological cell cannot survive as a close system, thereby molecules enter and leave the cell through the plasma membrane. A molecule or an ion that crosses the membrane (without input of metabolic energy) is transported passively by moving down a concentration or electrochemical gradient. This process is also called diffusion and is driven by the kinetic theory of matter. The kinetic energy of these particles is proportional to their temperature. This diffusion process is balanced within the system, and the flow of substances across the membrane occurs naturally. However, an artificial increase of that flow could be desirable for medical purposes including drug delivery.

In the present study we investigate the effects of a shock wave interacting with a biological membrane. A shock wave is defined as a sudden change (discontinuity) in pressure, density, particle velocity and internal energy. The more general term of *stress wave* has also been used [2]. The generation of shock waves by short laser pulses followed the invention of the Qswitched laser [3], while around the same time, the potentially deleterious effects of stress waves generated during medical applications of pulsed, high-power lasers were also demonstrated [4].

In the past, the effects of stress and shock waves on cells and tissue have been investigated in connection with ultrasonics, laser shock waves (LSW), acoustic extracorporeal shock waves (ESW) and laser–tissue interactions [2], and they have been further used in several fields of medicine such as kidney stone disintegration, orthopaedic surgery, brain neurosurgery and cancer treatment [5].

LSW, ESW, and ultrasound, can render the plasma membrane permeable [6] thus they can be used to increase the uptake of antibiotic agents into the cells. ESW chemotherapy, specifically,

DOI: 10.1002/fld

has been proposed as a promising method for cancer treatment [5]. LSW [7] also possesses many optical properties such as spatial and temporal coherency, minimum angular beam divergence, polarization and monochromaticity can also provide an alternative source of radiant energy of extremely high instantaneous power.

A number of studies have shown that high-energy shock waves are cytotoxic to tumour cells [8], enhance drug efficiency [9] and have chemotherapeutic effects in gene therapy and anticancer drug delivery [10, 11]. However, the detailed mechanism of cell permeabilization due to a shock wave still remains unknown. As cancer is one of the leading causes of death, finding ways to improve the effectiveness of anticancer drug delivery is of great interest. Cellular uptake of small polar molecules has been suggested to have beneficial role, e.g. potentiating the effects of cisplatin [12] and bleomycin [13] in cancer therapy. Other mechanisms by which shock waves may enhance chemotherapeutic effects are by increasing apoptosis and decreasing cell proliferation in the tumour tissue [14].

The aim of the present paper is to investigate by means of atomistic simulations the effects of the interaction of a shock wave with a biological membrane, on different membrane properties including thickness, area, volume, order parameter and lateral diffusion. The computational model for a shock wave interacting with a membrane is discussed in Section 2. Section 3 presents the results of the study and Section 4 summarizes the most important conclusions.

2. MOLECULAR DYNAMICS MODEL

2.1. Biological membrane model

The model is defined by a rectangular lattice of hydrated lipids, which consists of 21 555 atoms of 66 dalmitoyloleoylphosphatidylcholine (POPC) lipids forming the bilayer, and 4237 water molecules (Figure 2). The 3-D structure of the lipid molecule is defined by oxygen, nitrogen, carbon, hydrogen and phosphorous atoms highlighted in red, blue, pale blue, white and yellow colours, respectively. The same colour code is used for the water molecule, which is much simpler.

The lipid tails, pointing inward, were almost fully extended in order to reduce the required minimization time in the molecular dynamics (MD) simulations. The lattice period and actual surface density of lipid molecules were set to fit the distance between the layers and actual

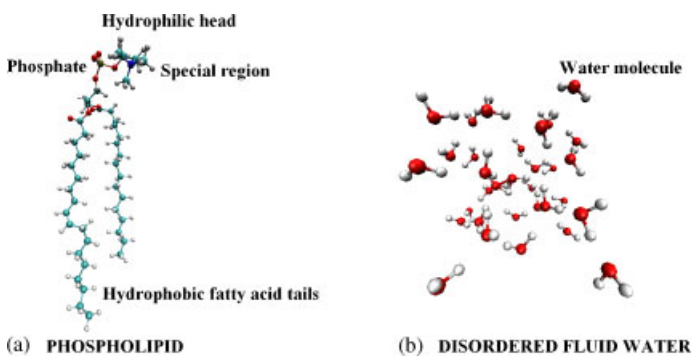

Figure 2. Molecular structure of the lipid molecule (a) and water (b).

DOI: 10.1002/fld

membrane thickness [15]. Both the parameters can be obtained through experiments [16] and are used to calculate the potential function of the molecules. The molecules are placed in an equilibrium position after the minimization process.

In order to generate a structure as realistic as possible, some disorder was introduced by placing each lipid in random orientation in the membrane plane with truncated Gaussian spread in the perpendicular direction. A short (1 ps) minimization in vacuum was conducted to eliminate the steric collisions among the lipid atoms [15].

Water molecules are built around the lipids one by one in order to properly hydrate the lipid head groups. All molecules outside the lipid dimensions and inside the hydrophobic layer are also deleted. The characteristics of water molecules are [15]:

1. Irregularly shaped solvent volumes, adapted to a given solute structure.
2. Minimal solute–boundary distance.
3. Disordered (fluid) water, not a grid of water molecules, i.e. ice.
4. Minimization of the positions of all water molecules.

2.2. Molecular dynamics method

In the present study, we have employed NAMD, a parallel MD code [17] designed for high-performance simulation of large biomolecular systems.[‡] NPT ensemble simulations of the hydrated lipid bilayer at 310 K have been performed in conjunction with periodic boundary conditions in order to avoid artefacts due to the presence of boundaries [18]. Dynamically adjusting the size of the unit cell and rescaling all atomic coordinates during the simulation can control the pressure that can be calculated from individual atoms.

In a system of N particles, the position, velocity and acceleration of the particles at time t are given by the 3-D vectors $r_i(t)$, $v_i(t)$ and $a_i(t)$, respectively, where i $(i = 1, 2, \ldots, N)$ is the particle index. Newton's equations in terms of the mass of each particle (m_i) and force applied to them (F_i) are written as

$$\begin{aligned} v_i &= \frac{\partial r_i}{\partial t} \\ a_i &= \frac{\partial v_i}{\partial t} = \frac{F_i}{m_i} \end{aligned} \tag{1}$$

The velocity Verlet integration method [19] is used to advance the positions and velocities of the atoms in time by solving a $6N$ first-order ordinary differential equation system:

$$\begin{aligned} r(t + \Delta t) &= r(t) + \Delta t \cdot v(t) + \tfrac{1}{2} \cdot \Delta t^2 \cdot a(t) + O(\Delta t^3) \\ v(t + \Delta t) &= v(t) + \tfrac{1}{2} \cdot \Delta t \cdot (a(t) + a(t + \Delta t)) + O(\Delta t^3) \end{aligned} \tag{2}$$

where Δt is the time step. Computation of the long-range, van der Waals and electrostatic interactions between every non-bonded pair of atoms in the system at every time step is computationally intensive. The local interactions (bonded, van der Waals and electrostatic interactions within a

[‡]NAMD was developed by the Theoretical and Computational Biophysics Group in the Beckman Institute for Advanced Science and Technology at the University of Illinois at Urbana-Champaign. Information about the code including validation studies can be found at www.ks.uiuc.edu/Research/namd.

DOI: 10.1002/fld

specified distance) are calculated at each time step, while the long-range interactions (electrostatic interactions beyond the specified distance) are computed every certain number of time steps thus reducing the computational cost and increasing the accuracy [11].

A smooth splitting function is used to separate a fast varying short-range portion of the electrostatic interaction from a more slowly varying long-range component [20]. As the fastest motions within the lipid bilayer, including diffusion and orientation correlation of water, occur on a timescale up to a few picoseconds [19], we have employed a time step equal to 1 femtosecond (fs). The non-bonded and full electrostatic interactions have been calculated every 2 and 4 fs, respectively.

2.3. Minimization

The minimization process adjusts the coordinates of the system in order to lower the energy. It is performed to relieve strain in conformations obtained either experimentally or by averaging of several structures [16]. For macromolecular systems, the number of local minima and the cost of computations prevent exhaustive search of the energy minimum, however, a local minimum in the neighbourhood of the X-ray structure can be generally examined.

Before the actual membrane simulations are performed, we carry out a MD simulation for some time in order to minimize the energy and reach the equilibrium range for all variables. The default minimizer uses a sophisticated conjugate gradient and line search algorithm [21]. The method of conjugate gradients is used to select successive search directions (starting with the initial gradient), which eliminate repeated minimization along the same directions. Along each direction, a minimum is first computed (rigorously bounded) and then converged upon by either a golden section search, or, when possible, a quadratically convergent method using gradient information [21]. This method takes the minimization history into account to determine the next step, while converges to the minimum energy and can produce larger coordinate shifts (see [16] for more information). The minimization protocol had been run for 50 ps in three steps:

1. Minimization for 2 ps.
2. Temperature and pressure increment for 3 ps.
3. Volume equilibration for 45 ps.

2.4. Shock wave modelling

Koshiyama *et al.* [21] suggested that shock waves may provide a way of introducing macromolecules and small polar molecules into the cytoplasm, and consequently may find applications in gene therapy and anticancer drug delivery. In their study each shock wave source generated a different shock waveform, so it is uncertain precisely which shock wave parameters were important for uptake of the fluorophore. They concluded that the impulse of the shock wave is defined as

$$\mathrm{Ip} = \int_0^{\mathrm{Rt}} P \, \mathrm{d}t \tag{3}$$

where Rt, the duration of the impulse rather than the peak pressure, is a dominant factor for increasing the diffusion into living cells and P stands for the instant pressure during the impulse time.

Therefore, a single shock wave, applied downwards to a part of the water layer, can be characterized by an impulse which can be expressed by a velocity, V_z, determined by the change in the

DOI: 10.1002/fld

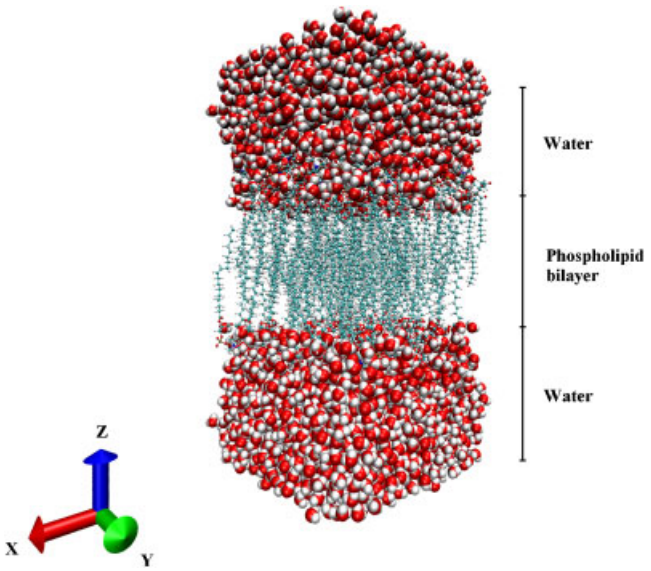

Figure 3. Molecular dynamics model.

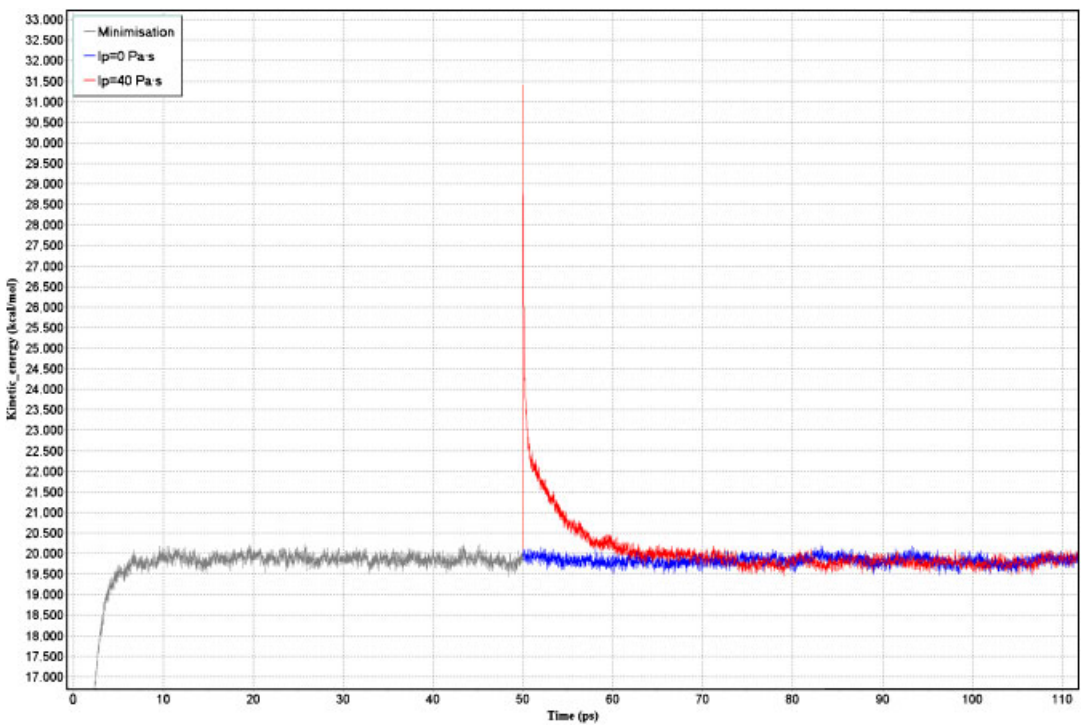

Figure 4. Kinetic energy variation in time during minimization and simulations corresponding to impulses of 0.0 and 40.0 Pa s, respectively.

DOI: 10.1002/fld

momentum in the upper water layer [21]:

$$V_z = \frac{\mathrm{Ip}}{M} \cdot A \tag{4}$$

where A and M are the area in the XY plane and the mass of model, respectively. Using (3), two simulations have been performed corresponding to impulses of 0.0 and 40.0 Pa s, respectively. As expected, the non-zero impulse will result in a jump of the kinetic energy at the beginning of the simulation (Figure 4).

3. MOLECULAR DYNAMICS SIMULATIONS

Because the stability of lipid bilayer systems is susceptible to initial conditions [22], prior to carrying out MD simulations (Figure 5) we performed a minimization simulation as discussed, ensuring that all the variables fluctuate around published values as the integration time increases.

For the case where no shock wave is applied the MD simulations (Figure 6) continue further for another 200 ps, following the minimization of 50 ps.

In the case where a shock wave is applied, the MD simulation starts using the latest co-ordinates and velocities of the atoms as obtained by the minimization simulation (Figure 7).

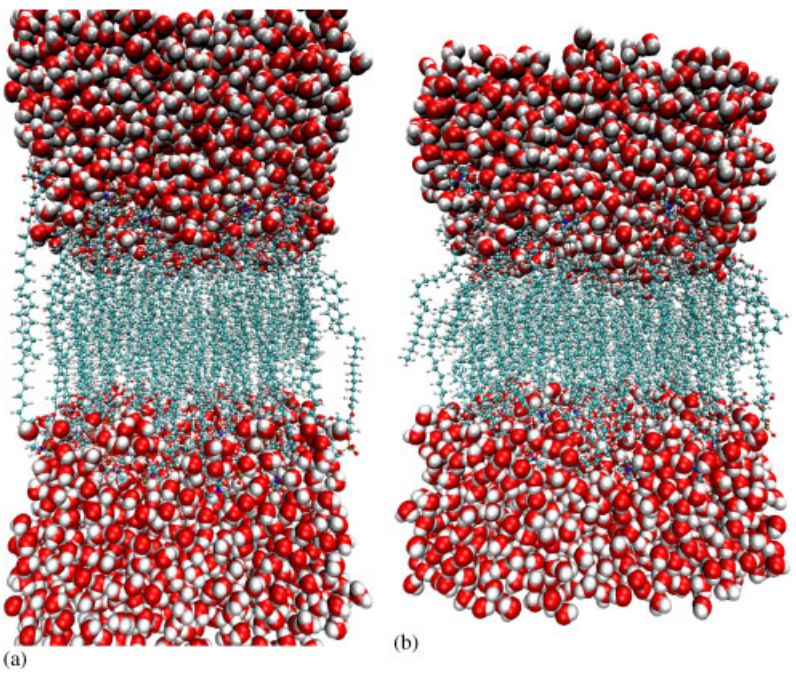

Figure 5. Molecular dynamics minimization: initial condition (a) and following minimization (b) approximately after 50 ps.

DOI: 10.1002/fld

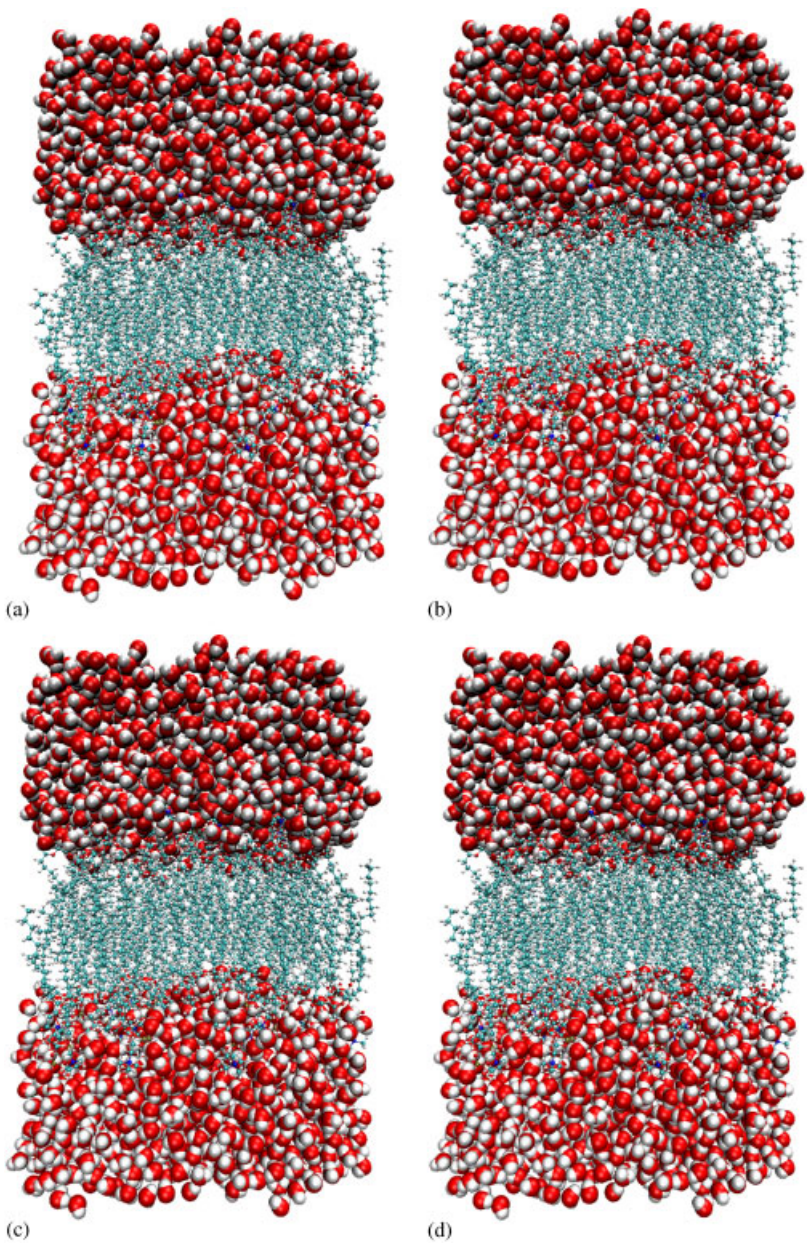

Figure 6. Molecular dynamics simulation without a shock wave: (a) $t = 0.1$ ps; (b) $t = 25$ ps; (c) $t = 50$ ps; and (d) $t = 75$ ps after minimization.

Fully hydrated lipid bilayers are not close to being in a crystalline state; hence, crystallography cannot be used to determine the bilayer structure by diffraction. The problem becomes even more difficult for bilayers which are in a fluid phase where the hydrocarbon chains are disordered in

DOI: 10.1002/fld

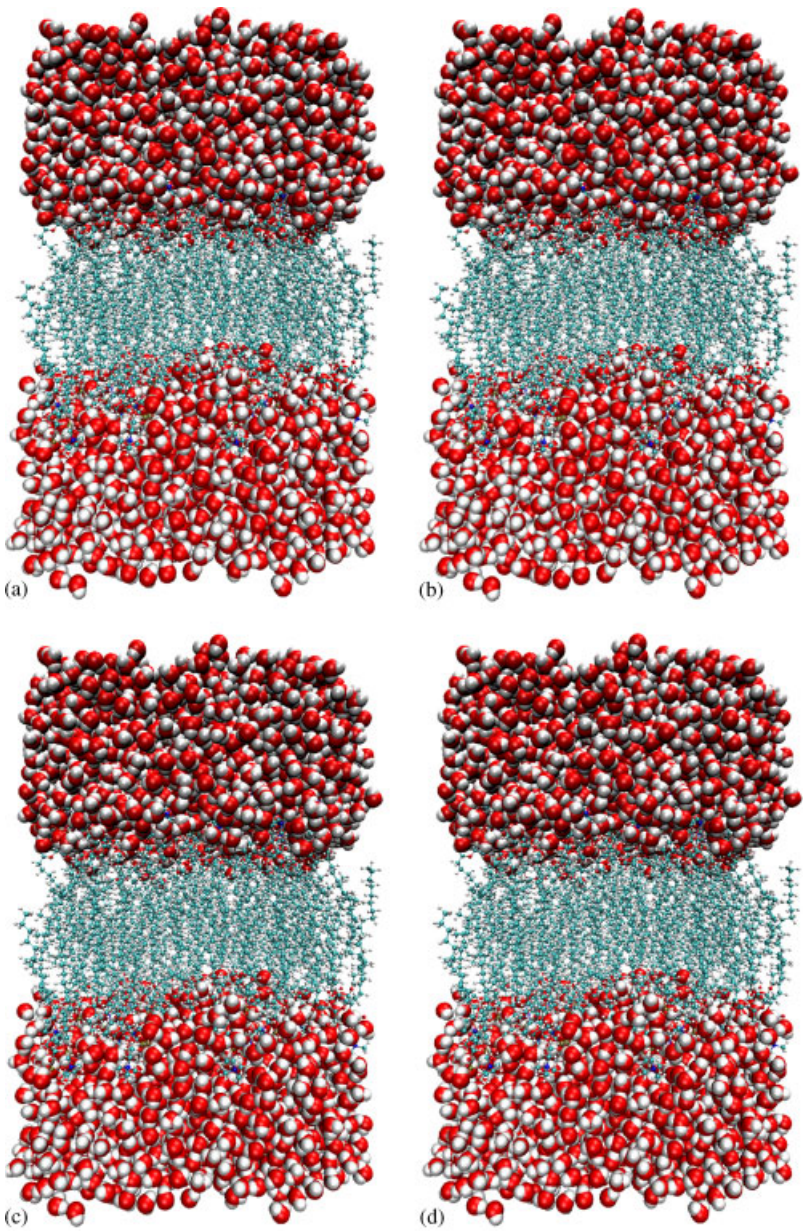

Figure 7. Molecular dynamics simulation when a shock wave (Ip = 40 Pa s) interacts with a lipid membrane: (a) $t = 0.1$ ps; (b) $t = 25$ ps; (c) $t = 50$ ps; and (d) $t = 75$ ps after minimization.

contrast to nearly fully extended lipid crystals. These differences are expected when there is much more water in fully hydrated lipid bilayers. Water alters the balance of interaction energies of the bilayers compared to the nearly dry crystalline state, and also allows bigger fluctuations [23].

DOI: 10.1002/fld

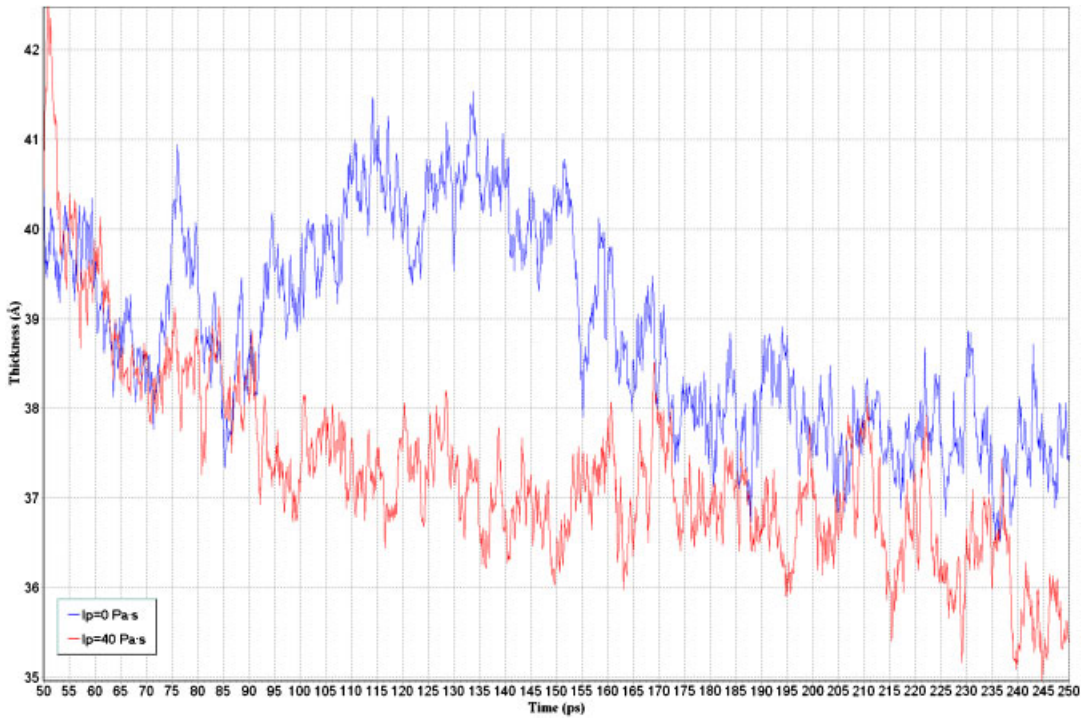

Figure 8. Lipid bilayer thickness for Ip = 40.0 and 0 Pa s.

According to the kinetic theory of matter, all the particles in a model must be in constant movement. Their positions, calculated by solving the equations previously exposed, change all along the simulation time, so, starting from a crystal structure, the fluid phase can be simulated using the MD.

3.1. Membrane thickness

The thickness of the membrane keeps changing all along the simulation as the particles are in continuous movement and the dimensions of the model vary. Thickness can be measured by calculating the difference between the maximum, $\max(r_{\text{lipid}}(t))$, and the minimum, $\min(r_{\text{lipid}}(t))$, positions of the lipid phosphorous atoms, i.e. $\max(rz_{\text{lipid}}(t)) - \min(rz_{\text{lipid}}(t))$.

The simulations show that when applying a shock wave the membrane gets thinner (Figure 8 and Table I).

3.2. Area per lipid and volume of the membrane

The area per lipid is the area of the lipid bilayer in the XY plane, calculated by $\text{Area}\,XY = [\max(rx_{\text{lipid}}(t)) - \min(rx_{\text{lipid}}(t))] \cdot [\max(ry_{\text{lipid}}(t)) - \min(ry_{\text{lipid}}(t))]$; its variation in time is shown in Figure 9.

Calculating the maximum, minimum, mean value and range of this variable and dividing them by the number of lipids, gives the values per lipid shown in Table II.

DOI: 10.1002/fld

Table I. Maximum, minimum and mean values of the lipid bilayer thickness for Ip = 40.0 and 0 Pa s.

Impulse (Pa s)	Ip = 0	Ip = 40
Maximum	41.54	42.48
Minimum	36.51	34.95
Mean value	38.87	37.30

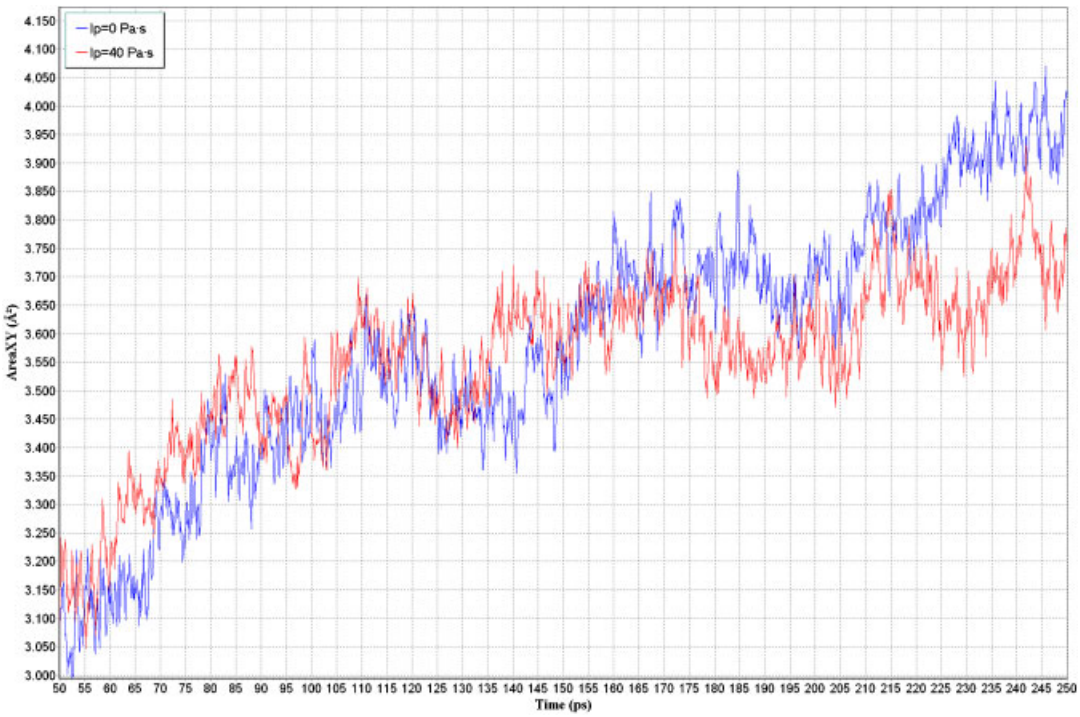

Figure 9. Area per lipid for Ip = 40.0 and 0 Pa s.

Table II. Maximum, minimum and mean values of the area per lipid.

Impulse (Pa s)	Ip = 0	Ip = 40
Maximum	61.67	59.57
Minimum	45.36	46.18
Mean value	54.23	53.79

The values for (Ip = 0) are in fair agreement with results from previous studies shown in Table III assuming that the values shown in the literature are mean values. The values are slightly lower as the membrane area will keep on increasing along the simulation. Our simulations show that the shock wave reduces the area in the *XY* plane.

DOI: 10.1002/fld

Table III. Comparison of structural parameter values of lipid bilayers taken from previously published computational and experimental studies [24].

	Area per lipid (Å^2)	Thickness (Å)
Simulation	64 ± 1	38 ± 1
Experiment	63–66	35–41
Present	62 (max), 54 (mean)	42 (max), 39 (mean)

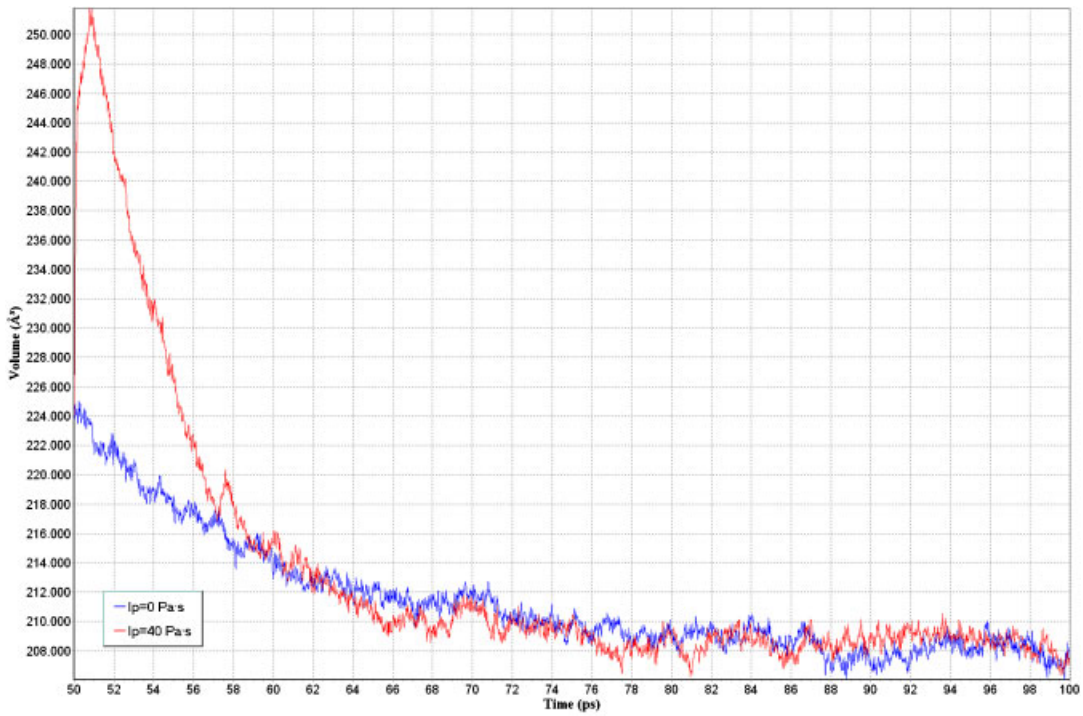

Figure 10. Volume of the membrane model for Ip = 40.0 and 0 Pa s.

When the shock wave is applied, the volume of the membrane model increases since the velocity of the particles is affected by the impulse. However, following the transient change, the volume gradually reduces and eventually returns to an equilibrium state (Figure 10).

3.3. Order parameter

The deuterium-order parameter (Scd) gives a measure of the average methylene group orientation with respect to the bilayer normal. It can be calculated in MD simulations using

$$\mathrm{Scd} = \tfrac{1}{2} \cdot (3\,\mathrm{Cos}(\beta) - 1) \tag{5}$$

DOI: 10.1002/fld

Table IV. Maximum, minimum and mean values for the absolute value of the order parameter.

Impulse (Pa s)	Ip = 0	Ip = 40
Maximum	0.2317	0.2342
Minimum	0.1851	0.1902
Mean value	0.2038	0.2079

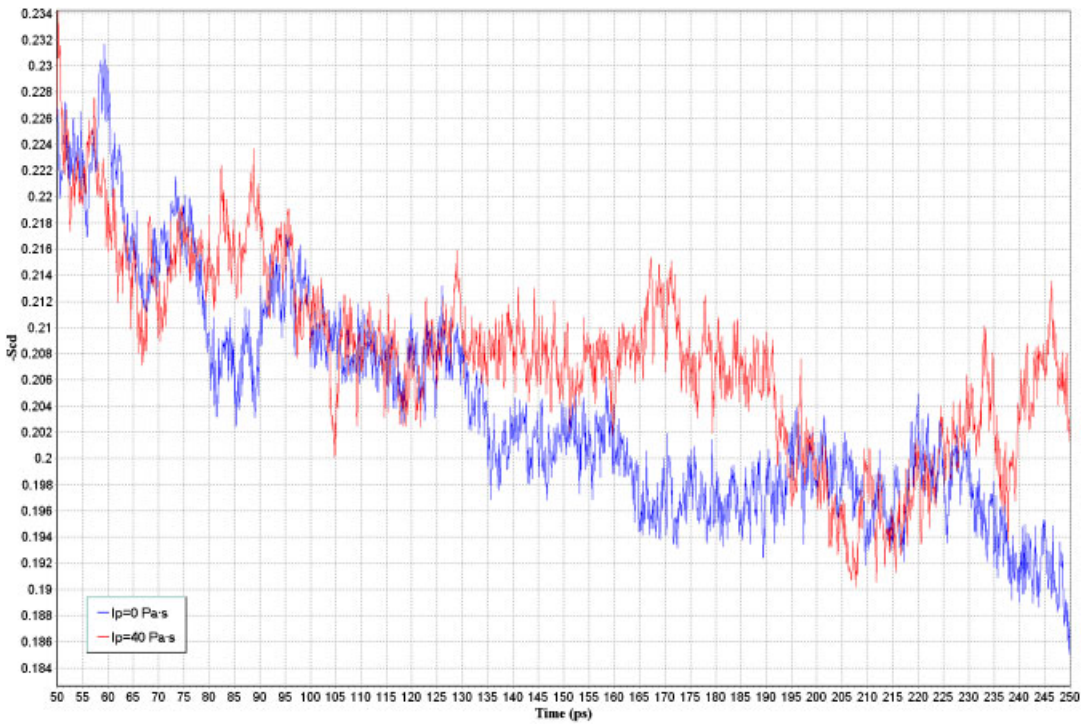

Figure 11. Order parameter variation for Ip = 40.0 and 0 Pa s.

where β is the angle between a vector normal to the bilayer and the plane formed by the carbon and deuterium atoms. The Scd has been calculated for all lipids along the integration time (Figure 11).

The values obtained for a lipid membrane without applying a shock wave are also in fair agreement with previous simulation results. Scd $= -0.27 \pm 0.01$ [25].

When applying a shock wave the disorder increases, thereby |Scd| becomes slightly larger (Table IV).

3.4. Lateral diffusion

Lateral diffusion in lipid membranes has been extensively studied in the past, however, the mechanism by which lipids diffuse is not yet well understood [26]. The biological cell membrane consists of a fluid lipid bilayer with the lipids moving through the membrane surface. The centre of mass

DOI: 10.1002/fld

Table V. Calculated diffusion values for Ip = 40.0 and 0 Pa s.

Impulse (Pa s)	Ip = 0	Ip = 40
Diffusion (10^{-7} cm^2/s)	9.8	12.8

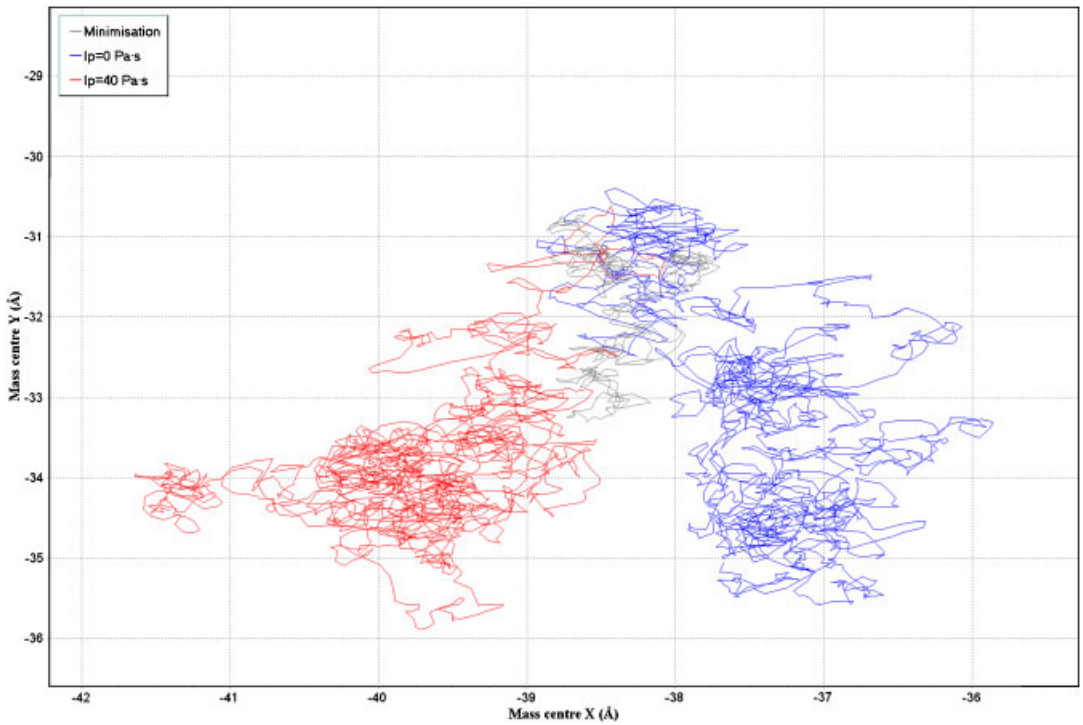

Figure 12. Mass centre of the lipids trajectory.

of the lipids trajectory in the simulated membrane has been traced and this is plotted in Figure 12 for Ip = 40.0 and 0 Pa s.

During the simulation, the fluid–lipid membrane can experience motion of the entire bilayer with respect to the centre of mass of the system (that also includes the water), and even motion of the two monolayers with respect to each other [27]. This behaviour of the lipids implies a lateral motion, which can be quantified through the long-time mean square distance coefficient (msd) yielding a diffusion coefficient D, which is defined by

$$D = \lim_{t\to\infty} \frac{1}{2 \cdot d_f} \cdot \frac{\mathrm{d}}{\mathrm{d}t}[r_i(t) - r_i(0)]^2 \tag{6}$$

where d_f is the number of dimensions in which the diffusion is measured ($d_f = 2$ for lateral diffusion) and D is the computed diffusion coefficient that is obtained from the slope of msd using linear regression analysis: msd = Initial msd + slope · time. The diffusion values obtained from

DOI: 10.1002/fld

the above equation are listed in Table V, and for the case $Ip = 0$ Pa s the diffusion value is of the same order of magnitude as the ones reported. $D = 4.5 \times 10^{-7}$ cm^2/s [25]. The results show that application of the shock wave results in an increase of the membrane's diffusion coefficient.

4. CONCLUDING REMARKS

We presented molecular dynamics (MD) modelling of a shock wave interacting with a biological membrane and examined the effects of an impulse on the lipid bilayer membrane system. MD simulations provide a unique tool to analyse biomembrane properties from an atomistic perspective.

Several properties of the cell membrane, both when applying a shock wave and without a shock wave being imposed, have been calculated. A fair agreement was found between the present MD simulations and previously published data for lipid membranes (without a shock wave). When a shock wave is applied the membrane thickness and area per lipid are slightly reduced; the order parameter is slightly increased; and most importantly the diffusion coefficient is also increased. The latter shows that the implementation of a shock wave can make the cell membrane transiently more permeable.

ACKNOWLEDGEMENTS

The financial support from the HEAL Cancer Charity is greatly acknowledged.

REFERENCES

1. Singer SJ, Nicolson GL. The fluid mosaic model of the structure of cell membranes. *Science* 1972; **172**:720–731.
2. Lee S, Doukas AG. Laser-generated stress waves and their effects on the cell membrane. *IEEE Journal of Selected Topics in Quantum Electronics* 1999; **5**:997–1003.
3. Carome EF, Clark NA, Moelle CE. Generation of acoustic signals in liquids by ruby laser-induced thermal stress gradients. *Applied Physical Letters* 1964; **4**:95–97.
4. Fine S, Klein E, Nowak W, Scott RE, Laor Y, Simpson L, Crissey J, Donoghue J, Deer VE. Interaction of laser radiation with biological systems I. Studies of interactions with tissues. *Federation of Societies for Experimental Biology* 1965; **24**:S35–S45.
5. Takayama K. Applications of shock wave research to medicine. *Shock Wave Journal* 1999; **2010**:23–32.
6. Mulholand SE, Lee S, McAuliffe DJ, Doukas AG. Cell loading with laser-generated stress waves: the role of the stress gradient. *Pharmaceutical Research* 1999; **16**:514–518.
7. Cleary SF. Laser pulses and the generation of acoustic transients in biological material. *Laser Applications in Medicine and Surgery* 1977; **3**:175–219.
8. Russo P, Stephenson RA, Mies C, Huryk R, Heston WD, Melamed MR, Fair WR. High energy shock waves suppress tumor growth *in vitro* and *in vivo*. *Journal of Urology* 1986; **135**(3):626–628.
9. Gambihler S, Delius M, Ellwart JW. Permeabilization of the plasma membrane of L1210 mouse leukemia cells using lithotripter shock waves. *Journal of Membrane Biology* 1994; **141**:267–275.
10. Worle K, Steinbach P, Hofstadter F. The combined effects of high energy shock waves and cytostatic drugs or cytokines on human bladder cancer cells. *British Journal of Cancer* 1994; **69**(1):58–65.
11. Allen MP, Tildesley DJ. *Computer Simulation of Liquids*. Oxford University Press: Oxford, England, 1987.
12. Weiss N, Delius M, Gambihler S, Eichholtz-Wirth H, Dirschedl P, Brendel W. Effect of shock waves and cisplatin on cisplatin-sensitive and -resistant rodent tumors *in vivo*. *International Journal of Cancer* 1994; **58**:693–699.
13. Kambe M, Ioritani N, Shirai S, Kambe K, Kuwahara M, Arita D, Funato T, Shimodaira H, Gamo M, Orikasa S, Kanamaru R. Enhancement of chemotherapeutic effects with focused shock waves: extracorporeal shock wave chemotherapy (ESWC). *In Vivo* 1996; **10**:369–375.
14. Kato M, Ioritani N, Suzuki T, Kambe M, Inaba Y, Watanabe R, Sasano H, Orikasa S. Mechanism of anti-tumor effect of combination of bleomycin and shock waves. *Japan Journal of Cancer Research* 2000; **91**(10):1065–1072.

DOI: 10.1002/fld

15. Humphrey W, Dalke A, Schulten K. VMD—visual molecular dynamics. *Journal of Molecular Graphics* 1996; **14**:33–38.
16. Brooks BR, Bruccoleri RE, Olafson BD, States DJ, Swaminathan S, Karpus M. CHARMM: a program for macromolecular energy, minimization and dynamics calculations. *Journal of Computational Chemistry* 1983; **4**:187–217.
17. Phillips JC, Braun R, Wang W, Gumbart J, Tajkhorshid E, Villa E, Chipot C, Skeel RD, Kale L, Schulten K. Scalable molecular dynamics with NAMD. *Journal of Computational Chemistry* 2005; **26**:1781–1802.
18. Tieleman DP, Marrink SJ, Berendsen HJC. A computer perspective of membranes: molecular dynamics studies of lipid bilayer systems. *Biochimica et Biophysica Acta* 1997; **1331**:235–270.
19. Spreiter Q, Walter M. Classical molecular dynamics simulation with the velocity Verlet algorithm at strong external magnetic field. *Internal Report*, Institut für Theoretische Physik II, University of Erlangen-Nuremberg, Germany, 1998.
20. Bhandarkar M, Brunner R, Chipot C, Dalke A, Dixit S, Grayson P, Gullingsrud J, Gursoy A, Hardy D, Humphrey W, Hurwitz D, Krawetz N, Nelson M, Phillips J, Shinozaki A, Zheng G, Zhu F. NAMD User's Guide. *Internal Report*, Theoretical Biophysics Group, University of Illinois and Beckman Institute, 2003.
21. Koshiyama K, Kodama T, Hamblin MR, Doukas AG, Yano T, Fujiyama S. Molecular delivery into a lipid bilayer with a single shock wave using molecular dynamic simulation. *Conference Proceedings*, vol. 754. American Institute of Physics: New York, 2005; 104–106.
22. Husslein T, Newns DM, Pattnaik PC, Zhong QF, Moore PB, Klein ML. Constant pressure and temperature molecular-dynamics simulation of the hydrated diphytanolphosphatidycholine lipid bilayer. *Journal of Chemical Physics* 1998; **109**:2826–2832.
23. Nagle JF, Tristram-Nagle S. Structure of lipid bilayers. *Biochimica et Biophysica Acta* 2000; **1469**:159–195.
24. Pasenkiewicz-Gierula M, Murzyn K, Rog T. Molecular dynamics simulation studies of lipid bilayer systems. *Acta Biochimica Polonica* 2000; **47**(3):601–611.
25. Rog T, Murzyn K, Pasenkiewicz-Gierula M. Molecular dynamics simulations of charge and neutral lipid bilayers: treatment of electrostatic interactions. *Acta Biochimica Polonica* 2003; **50**:789–798.
26. Moore PB, Lopez CF, Klein ML. Dynamical properties of a hydrated lipid bilayer from a multinanosecond molecular dynamics simulation. *Biophysical Journal* 2001; **81**:2484–2494.
27. Hofsäß C, Lindahl E, Edholm O. Molecular dynamics simulations of phospholipid bilayers with cholesterol. *Biophysical Journal* 2003; **84**:2192–2206.

DOI: 10.1002/fld